

Rapeseed Oil-Based Polyurethane Foams Modified with Glycerol and Cellulose Micro/Nanocrystals

Mirna A. Mosiewicki,¹ Piotr Rojek,² Sławomir Michałowski,² Mirta I. Aranguren,¹ Aleksander Prociak²

¹Institute of Materials Science and Technology (INTEMA), University of Mar del Plata, National Research Council (CONICET), 7600 Mar del Plata, Argentina

²Department of Chemistry and Technology of Polymers, Cracow University of Technology (CUT), 24 Warszawska, 31-155 Cracow, Poland

Correspondence to: M. Mosiewicki (E-mail: mirnamosiewicki@hotmail.com)

ABSTRACT: A rapeseed oil-based polyol (ROPO) was synthesized using chemical modification of the rapeseed oil (RO) by epoxidation reaction followed by oxirane ring-opening with diethylene glycol. The ROPO was used in the formulation of low-density green polyurethane (PU) foams. The use of glycerol as hydroxyl component, water as a reactive blowing agent and micro/nanocellulose (MNC) as a reinforcement increases the content of natural components in the formulations with important effects on the final foam properties. The ROPO and their intermediate products are characterized by analytical techniques and FTIR spectroscopy, while the final PU foams are characterized by morphological and mechanical analysis. The results show that the addition of glycerol increases the modulus and yield stress. The incorporation of MNC in small amounts is enough to increase the modulus at low temperatures. Both modifiers cause an increase in water absorption and the fragility of the cell walls, reflected in the micrographs of the foams. © 2014 Wiley Periodicals, Inc. *J. Appl. Polym. Sci.* **2015**, *132*, 41602.

KEYWORDS: cellulose and other wood products; foams; polyurethanes; synthesis and processing

Received 8 August 2014; accepted 6 October 2014

DOI: 10.1002/app.41602

INTRODUCTION

Polyurethanes (PUs) are polymers with ample range of properties and areas of application. Among those, they can be produced as low-density flexible foams, which are mostly known for being used in mattresses and cushioning, or low-density rigid foams used to manufacture thermal insulation panels. Different types of high-density flexible PU foams can be used in shoe-soleing or as structural foams, while nonfoamed PUs are used in areas such as construction, transport, aerospace.^{1–3}

Nowadays, the most common raw materials for PUs are supplied by the petroleum industry. Because of the uncertain future availability of petroleum, scientists all over the world are searching for alternative bio-based raw materials. The PUs are generally prepared through the reaction between compounds with two or more reactive hydroxyl groups per molecule (diols or polyols) and isocyanates with more than one reactive group per molecule (diisocyanates or polymeric isocyanates). The use of vegetable oil based polyols is an interesting alternative because of the broad availability worldwide, relatively low cost, and potential biodegradability. The application of renewable raw materials for chemical synthesis may contribute to the reduction of the environmental impact, such as the consumption of non-renewable resources and the greenhouse gas emission. Moreover,

the hazards of chemicals should also be taken into account in order to reduce the impact of eco-toxicity.^{4,5}

Vegetable oils consist of triglyceride molecules (glycerol covalently linked to three fatty acid chains). They present many reactive sites, which are able to be chemically modified in order to achieve products that are useful for the polymer industry.⁶

Vegetable oils contain both types of fatty acids: saturated with non-reactive aliphatic chains (stearic or palmitic acids) and unsaturated, with aliphatic chains containing double bonds (oleic, linoleic, linolenic, ricinoleic acids). These natural compounds are of interest since various reactions can be performed onto their different groups in order to obtain bio-based polyols for PUs synthesis.⁴

Specifically, rapeseed oil (RO) is an edible oil that includes unsaturated acids in its structure (around 61% of oleic acid, 21% of linoleic acid, 8% of linolenic acid, and others 10%) able to be chemically modified to introduce hydroxyl groups.⁷ The polyol functionality and the resulting crosslinking density of the derived PUs are related to the double bond content in the natural oils.^{7,8}

Different paths of reaction of the triglyceride double bonds for incorporating hydroxyls groups have been studied.^{4,6,9–12} The structure of resulting oil-based polyol depends on the selected modification method and the chosen vegetable oil (vegetable

oils differ in the amount, distribution, and position of the carbon-carbon double bonds in the fatty acid chains). Moreover, the fatty acid profiles of the starting oils and the degree of oligomerization during polyol synthesis have important influence on the properties of PU products.¹³

Besides the diols or polyols, the production of PU foams requires the use of isocyanates and several additives (catalyst, blowing agent, surfactant, etc.) not always environmentally friendly. The use of water as reactive blowing agent offers the additional advantage of accelerating the reaction without the need of adding volatile organic compounds. On the other hand, the use of natural fibers as reinforcing material is an attractive alternative, since they have low cost and are available from renewable resources, reducing environmental concerns.^{14,15} The natural-fiber-reinforced foamed materials have also considerable importance in the automotive industry, because of the possibility of additionally reducing the weight of vehicles by virtue of the cellular structure that characterizes these type of fibers.¹⁶

In the last years, several studies have reported the results of cellular materials reinforced or filled with different types of fibers, which lead to changes in the polymer matrix behavior, such as the heat released during the polymerization reaction, the stiffness of the foams, the capacity of energy absorption, and their density among others.¹⁷⁻²⁴

The foam architecture obviously depends on the filler dispersion in PU system, and the cell-wall width compared to the particle size.²⁵

Some authors have reported the use of oil based polyols in PUs foam formulations²⁵⁻²⁸ with similar properties to those of petrochemical origin. Although there are some results on reinforced foams, the use of cellulose micro/nanoparticles in foams has not been much considered.

In this work, technical raw materials were applied in the oil-based polyol synthesis. The epoxidation of RO was carried out without any solvent (as it has been previously reported [11]) in order to simplify the method of the bio-polyol preparation and facilitate its application on industrial scale. The modified RO, together with different concentrations of glycerol were used as polyols in the preparation of rigid foams. Low amounts of MNC were also incorporated to the PU formulation in order to modify physical and mechanical properties of prepared foams.

EXPERIMENTAL

Materials

Nonrefined RO (provided by Organika Nowa Sarzyna) was used in the synthesis of a bio-polyol by epoxidation reaction using peracetic acid generated "*in situ*" as a result of the reaction of hydrogen peroxide (50 wt %, provided by Organika Nowa Sarzyna) and acetic acid (80 wt %, provided by Organika Nowa Sarzyna), followed by oxirane ring-opening with diethylene glycol (Sigma-Aldrich). Different additives were incorporated to the bio-polyol: surfactant agent (L6900, Momentive Performance Materials), catalyst (Polycat 5, Air Products and Chemicals) and water that was used as a reactive blowing agent. Glycerol (POCH, Gliwice) was added as a reactive triol to the polyol premix. Additionally, a commercial micro/nanocellulose,

MNC (Arbocel UFC-100, Rettenmaier) with an average fiber length of 8 μm and an average fiber thickness of 2 μm , was also incorporated to the rapeseed oil-based polyol (ROPO) premix.

The polyol premix was reacted with polymeric diphenylmethane diisocyanate (PMDI, provided by Minova Ekochem SA).

Synthesis of Rapeseed Oil Based Polyol

Epoxidation Reaction. The nonrefined RO was epoxidized using peracetic acid generated "*in situ*" as a result of the reaction of hydrogen peroxide and acetic acid. The temperature of the reaction mixture was kept in a range of 60–65°C. The final mixture forms two phases that are separated. The oily phase was washed several times until neutral pH.

Opening of the Oxirane Rings in Epoxidized Oil. Epoxidized rapeseed oil (ERO) was converted to polyol using diethylene glycol in stoichiometric molar ratio to epoxy groups. The temperature was kept at 95°C for 2.5 h.

A scheme of the chemical reaction steps is presented in Figure 1.

Foam Production

The components of the PU foam were mixed at room temperature in a plastic container, poured to the mold and let foaming in a free-rising process in a horizontal direction, while vertical rise was limited by the mold to 50 mm. The ROPO, catalyst (1.5 wt %), surfactant (1.3 wt %), water as blowing agent (5.3 wt %), and PMDI were the components of the basic formulation. All percentages are reported with respect to the total weight of polyols.

This basic formulation was modified by replacing the RO polyol with glycerol using the following glycerol/ROPO weight ratios: 0/100, 1/99, 3/97, and 5/95. The isocyanate index (moles of NCO groups/moles of OH groups) was adjusted to 1.1 for each system. A second set of samples were prepared by incorporating a commercial micro/nanocellulose (MNC) to the base ROPO/PMDI formulation as a filler to increase the natural components in the foam and to evaluate its effect on the final properties of the foams. Cellulose contents of 1, 2, and 3 wt % with respect to the total mass of the reaction mixture were added to the polyol premix.

In all the cases, the PMDI was rapidly added to the polyol premix containing the other components. The mixture was stirred for 10 s and then it was left to react and foam in the horizontal direction.

Polyol Characterization

The RO, ERO, and ROPO were characterized using analytical techniques (hydroxyl value, acid value, iodine value, epoxy value, and water content).²⁹

Fourier transform infrared (FTIR) spectra were recorded by the attenuated total reflection (ATR) method using a Thermo Scientific Nicolet 6700 FTIR spectrometer. The spectra were recorded over the range 500–4000 cm^{-1} with a resolution of 2 cm^{-1} and averaged over 32 scans.

Foam Characterization

The Foam Qualification System, FOAMAT was used to measure different physical parameters during foam formation

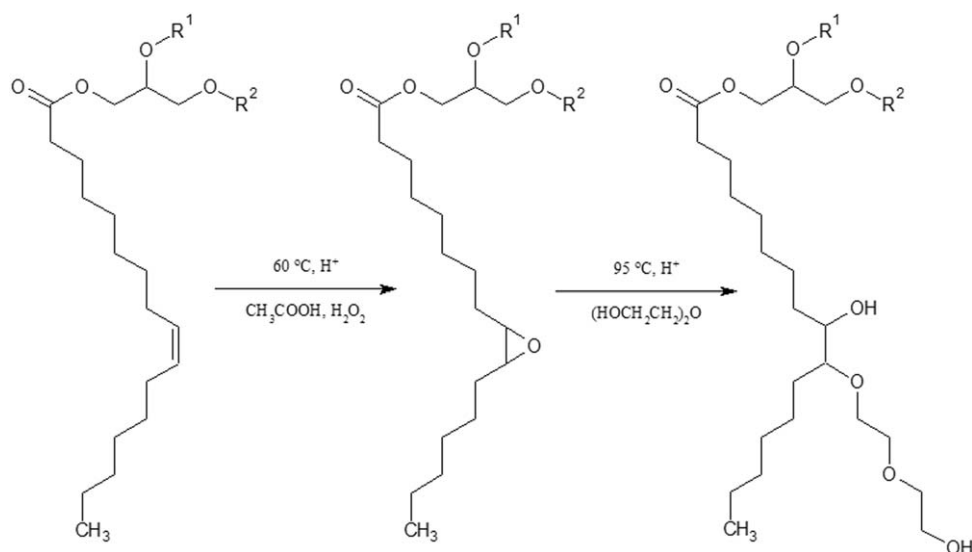


Figure 1. Chemical reaction steps to produce rapeseed oil based polyol.

[temperature, pressure, dielectric polarization (DP), and rise height of the foam].

Apparent density was calculated as the ratio between the weight and the volume of a cubic specimen ($50 \times 50 \times 50 \text{ mm}^3$). At least five replicated specimens of each sample were measured. To take the most representative part of the samples, the cubes were cut from the center of the foam (according to the Standard ISO 845).

Thermal conductivity tests were carried out using a Laser Comp Heat Flow Instrument Fox 200 (USA). The measurements were made according to the Standard ISO 8301 at an average temperature of 10°C (temperature of cold plate at 0°C and warm plate at 20°C).

Water absorption (volume %) after 24 h of immersion was determined for samples of $50 \times 50 \times 25 \text{ mm}^3$ according to ISO 2896 Standards.

Closed cell content (vol %) was estimated according to the Standard ISO 4590.

Morphological characterization was evaluated using an optical microscope with video channel. The average cross-section area and number of cells as well as the value of the anisotropy index were calculated using a specific software. Besides, a scanning electron microscope (SEM) Philips model SEM 505 operated at

15 kV was used to obtain photographs. Small specimens were cut from the middle of the foams in the direction of growth. Samples were sputter-coated with gold prior to SEM observation.

Dynamic mechanical tests of the samples containing MNC were determined using an Anton Paar, Physica MCR rheometer. Torsion geometry was used with solid rectangular samples of length 30 mm, width 10 mm, and thickness 2 mm. Measurements were performed as temperature sweeps at a heating rate of $10^\circ\text{C}/\text{min}$, frequency of 1 Hz, and applied deformation of 0.1%, to ensure working in the linear viscoelastic range.

Compression tests were carried out using a Zwick Z005 TH Allround-Line equipment according to ISO 844. Specimens of $50 \times 50 \times 50 \text{ mm}^3$ were cut and tested at a crosshead speed of 5 mm/min. The compressive force was applied parallel and perpendicular to the growth direction in the foams. Four specimens of each sample were tested and the average values are reported.

Table I. Properties of the Rapeseed Oil (RO), Epoxidized Rapeseed Oil (ERO), and Rapeseed Oil Polyol (ROPO)

	RO	ERO	ROPO
Hydroxyl value (mg KOH/g)	0	76.6	264.2
Water content (%)	0.12	0.40	0.66
Epoxy value (mol/100 g)	-	0.26	0
Iodine value ($\text{g I}_2/100\text{g}$)	109.7	3.2	-
Acid value (mg KOH/g)	3.47	4.88	7.60

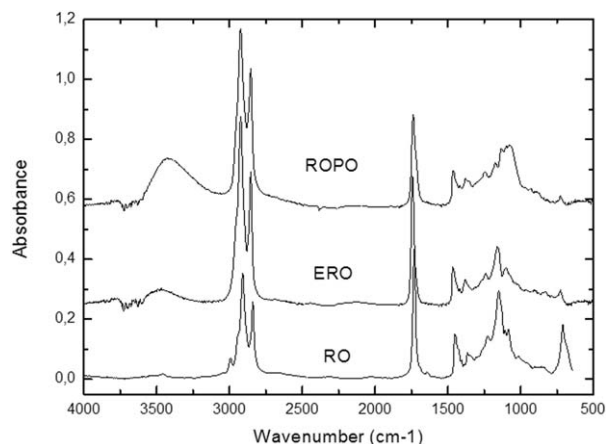


Figure 2. FTIR spectra of the RO, ERO, and ROPO.

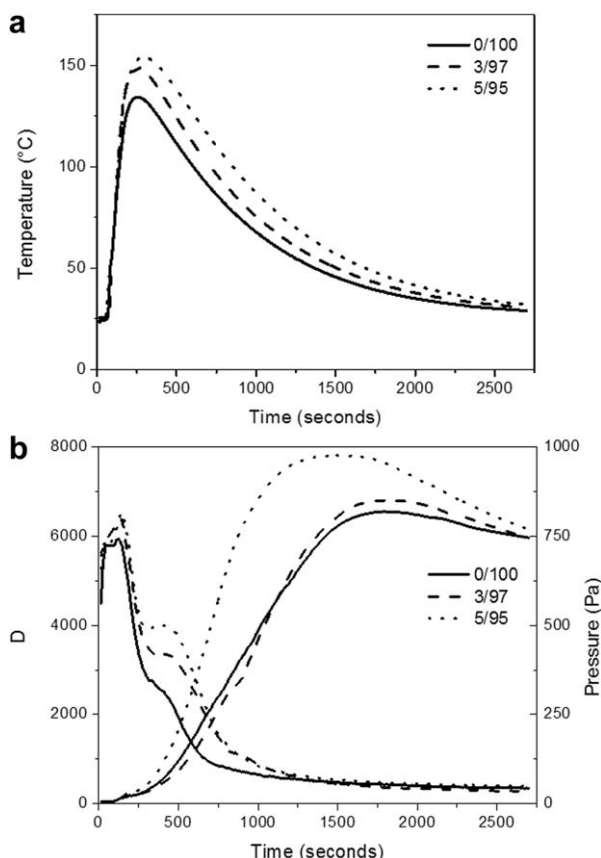


Figure 3. FOAMAT results. Temperature (a), pressure and dielectric polarization (b) variation as a function of time during foam preparation for the formulations with glycerol/rapeseed oil polyol weight ratios: 0/100, 3/97, and 5/95.

RESULTS

Characterization of the RO, ERO, and ROPO

Table I summarizes the results of the analytical techniques used to characterize the RO, ERO, and ROPO. The unmodified RO has no hydroxyl groups and very little amount of free acids. The iodine value of the unmodified RO denotes the presence of carbon–carbon unsaturations, corresponding to a functionality close to 4 per triglyceride molecule. After the epoxidation reaction, the epoxy value of the resulting product was 0.26 mol/100 g and the hydroxyl value 76.7 mg KOH/g, which is attributed to the fact that some of epoxy ring opening with water occurs during this step. As it was expected the iodine

value (which measures the content of C=C groups) decreases significantly because of the reaction of the carbon–carbon double bonds. After the second step of reaction, the ROPO had a hydroxyl value high enough for the preparation of rigid or semirigid foams.

Figure 2 shows the comparison of the FTIR spectra of the RO, ERO, and ROPO. The FTIR spectrum of the RO presents a peak at 3007 cm^{-1} corresponding to C=C bonds absorption, in agreement with the iodine value reported in Table I. The peak at 1745 cm^{-1} keeps up a correspondence to the C=O bonds in ester groups from triglyceride molecules. In comparison, the ERO spectrum presents a weak absorption at $3400\text{--}3500\text{ cm}^{-1}$ in concordance with a not null value of hydroxyl number (Table I). This fact was related to the opening of the epoxy rings that proceeds mildly during the epoxidation step of the reaction, as it was aforementioned. It is also possible to note that the band at 3007 cm^{-1} disappeared in the ERO spectrum due to nearly fully epoxidation of C=C bonds in the triglyceride structure.

The most relevant difference observed in the ROPO spectrum is the important increase in the band intensity at 3430 cm^{-1} after the epoxy ring opening reaction corresponding to hydroxyl absorption, which is in agreement with the high hydroxyl number of this sample as reported in Table I. Another significant difference is the appearance of an absorption band at $1050\text{--}1150\text{ cm}^{-1}$ corresponding to the C–O–C groups from diethylene glycol and oil polyol oligomers.

Characterization of the Foams

Foam Rising Times. Figure 3 shows the temperature (a), pressure and dielectric polarization (b) variation as a function of time during foam preparation for the formulations with glycerol/ROPO weight ratios: 0/100, 3/97, and 5/95.

As it is known, the exothermal crosslinking reaction causes the temperature increase in the foam sample. Figure 3(a) shows that the highest temperature reached by the foams increases with the incorporation of glycerol in the formulation and appears at longer times. The difference in maximum temperature is related to the content of the glycerol that has higher functionality per unit of mass than the ROPO. This leads to the formation of more urethane bonds and consequently, to the increase of the overall reaction exotherm that increases the temperature of the mixture and the crosslinking density of the system. Substitution of ROPO with glycerol (of lower molar mass than the bio-polyol) in the reactive mixture increases the hydroxyl group concentration in the foam formulation and

Table II. Properties of the Foams Modified with Glycerol

Glycerol/ ROPO weight ratio	Apparent density (kg/m^3)	Thermal conductivity ($\text{mW/m}^2\text{K}$)	Water absorption (vol %)	Closed cell content (vol %)
0/100	39.9 ± 2.9	23.9 ± 0.7	1.48 ± 0.92	78.9 ± 2.7
1/99	39.0 ± 1.4	23.4 ± 0.7	1.58 ± 1.36	82.3 ± 2.7
3/97	39.3 ± 0.5	24.5 ± 0.7	3.06 ± 1.13	86.5 ± 1.8
5/95	39.8 ± 0.5	24.1 ± 0.8	2.07 ± 0.35	84.4 ± 2.4

Table III. Properties of the Foams Modified with Cellulose (MNC)

MNC (wt %)	Apparent density (kg/m^3)	Thermal conductivity ($\text{mW/m}^2\text{K}$)	Water absorption (vol %)	Closed cell content (vol %)
0	39.9 ± 2.9	23.9 ± 0.7	1.48 ± 0.92	78.9 ± 2.7
1	38.9 ± 1.4	22.9 ± 0.4	7.85 ± 0.33	83.3 ± 0.7
2	39.1 ± 1.6	23.5 ± 0.7	4.23 ± 1.69	80.5 ± 1.2
3	40.7 ± 3.0	23.1 ± 0.9	2.67 ± 0.26	82.5 ± 2.2

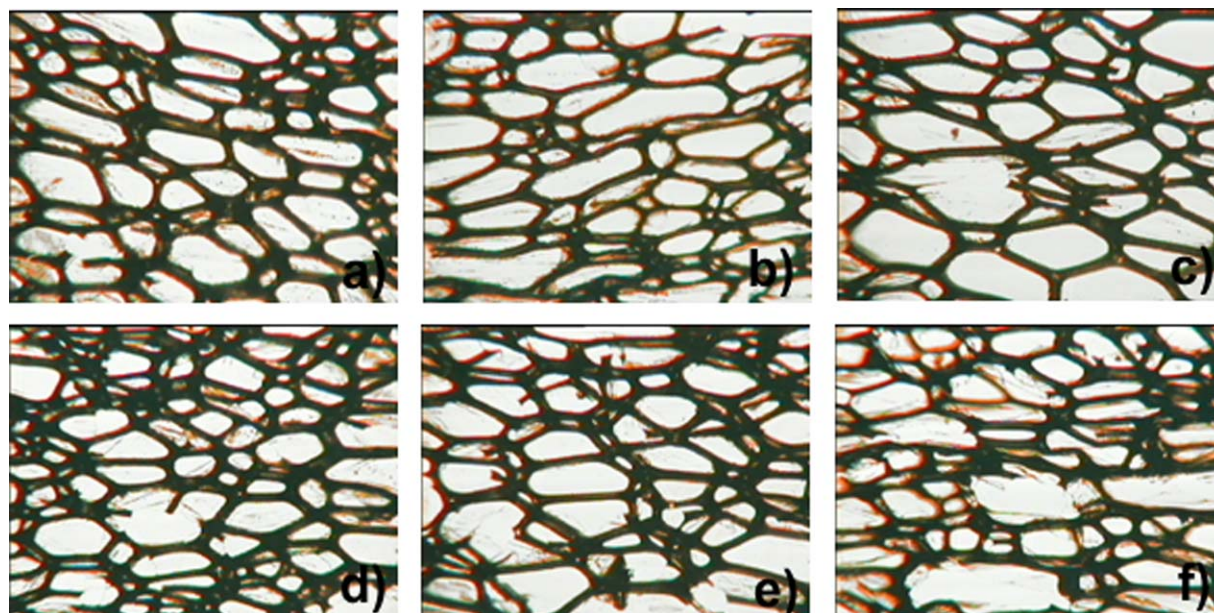


Figure 4. Transmission optical micrographs of foams. (a) Glycerol/ROPO = 0/100; (b) Glycerol/ROPO = 3/97; (c) Glycerol/ROPO = 5/95; (d) 1% MNC; (e) 2% MNC; (f) 3% MNC. [Color figure can be viewed in the online issue, which is available at wileyonlinelibrary.com.]

consequently, more PMDI is necessary to keep the same NCO/OH ratio. This fact causes that the formulations containing glycerol have a higher concentration of reactive groups per mass unit, which leads to higher heat release during reaction.

Figure 3(b) shows that the curves of pressure generated during foaming by the samples with 0 and 3 wt % of glycerol are quite similar during the measured time. However the sample with 5 wt % of glycerol present a curve of pressure that increases significantly at shorter times. The expanding foam presses the bottom of the expansion container where the pressure forces are measured. The rise curve reflects the dynamics of blowing agent generation (carbon dioxide) and it can also correspond to the evaporation of the water present in the system that occurs at shorter times as the glycerol content increases. This behavior can be related to two different facts: the higher temperature generated in the mixture with 5 wt % of glycerol [Figure 3(a)], which leads to higher gas pressure in cells because of the known direct correlation between temperature and pressure in the behavior of gases. The second main effect refers to the fact that as more glycerol is incorporated into the formulation, a higher concentration of crosslinking points is generated, which can also increase the total pressure of the system. As already mentioned, during foaming the expanding PU applies a stress on the bottom of the mold (where the sensor is located), and a material with higher crosslinking density could generate higher forces and consequently higher pressure on the mold.

Figure 3(b) also shows the curves of dielectric polarization as a function of time. The curves of dielectric polarization are used to determine resin curing.³⁰ Dielectric polarization is essentially determined by chain-like molecules with a large dipole moment due to their polar ends (groups OH and NCO). Chain formation precedes the crosslinking reaction that ultimately suppresses all dipole mobility during curing. All the dielectric

polarization curves show two steps at short times. The first DP decrease (at short times) is related mainly to the initial foam formation, so the decrease of apparent density. The second DP decrease is associated to formation of crosslinks.

As the percentage of glycerol increases in the composition, the DP increases at the beginning of the reaction associated with the fact that short glycerol molecules introduce higher dipole moment in comparison with the long chains of ROPO. At longer times, the curves display the final curing of the foam giving a constant signal after the chemical reaction is completed. As crosslinking begins and proceeds to the formation of a progressively less mobile, more rigid network, the capability of the molecules to be oriented by the applied electrical field progressively decreases. Thus, the dielectric polarization value decreases markedly when crosslinking begins and continues decreasing to the final immobilization of the molecules in the network. The more glycerol in the foam formulation, the more time the mixture needs to reach the final conversion. This is due to the higher initial concentration of —OH and —NCO groups in case of foams with glycerol. The higher percentage of glycerol, the higher DP slope is, meaning the faster crosslinking occurs.

Density, Closed Cell Content, and Thermal Conductivity

The physical properties of the foams containing different percentages of glycerol and those of the filled foams are presented in Tables II and III, respectively.

All the materials included in these two tables show comparable apparent densities and all the foams present relatively high percentage of closed cell contents (higher than 78%). The thermal conductivity shows negligible variation with the concentration of glycerol or cellulose.

Water absorption is also presented in Tables II and III. In general, the partial replacement of ROPO by glycerol, leads to the

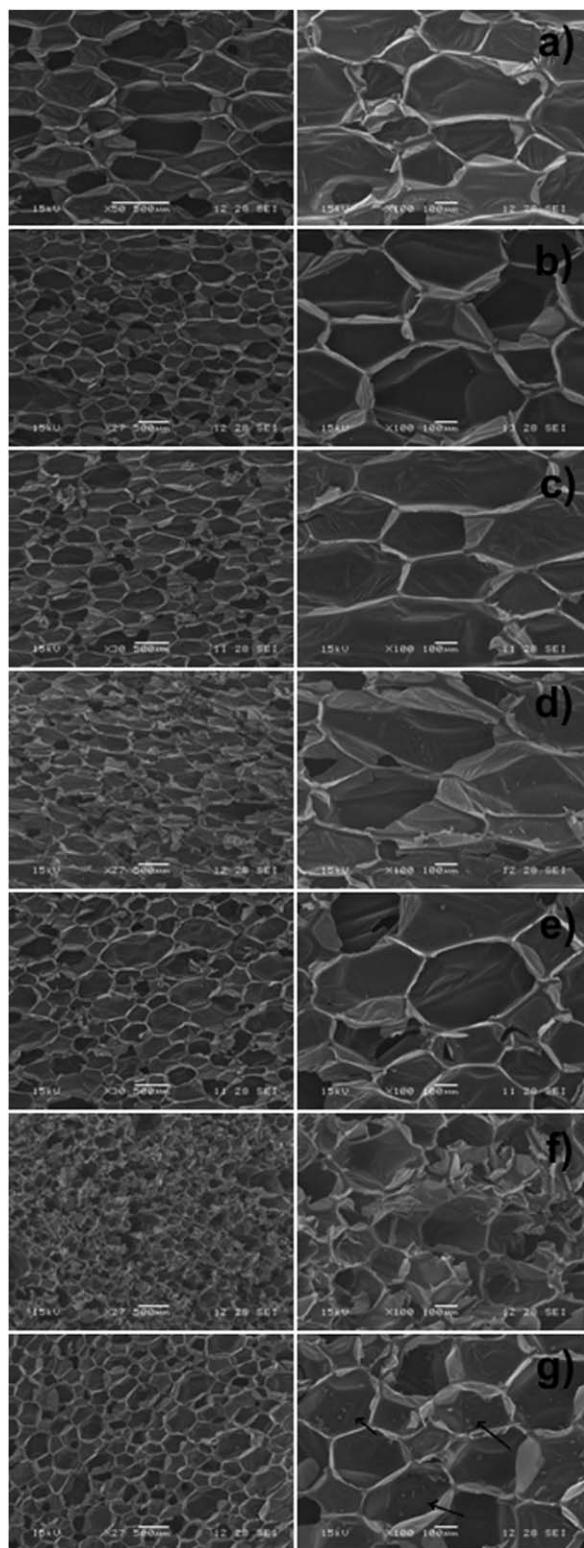


Figure 5. SEM micrographs of the foams. (a) Glycerol/ROPO = 0/100; (b) Glycerol/ROPO = 1/99; (c) Glycerol/ROPO = 3/97; (d) Glycerol/ROPO = 5/95; (e) 1% MNC; (f) 2% MNC; (g) 3% MNC.

increase of the water absorption with respect to the results obtained for the glycerol free foam (Table II). This fact could be associated to the more polar structures that are obtained when

ROPO is partially replaced with glycerol. Besides, the addition of MNC to the original formulation increases significantly the water absorption of the foams. In general, this fact could be associated to the hydroxyl groups in the MNC that stay unreacted after foam curing, remaining free to interact with water molecules during the immersion test. However, it can be noticed that the sample with 1 wt % of MNC presents a maximum in water absorption. As more MNC is added, filler can agglomerate with a high degree of particle–particle interactions, with decreased surface exposition of nonreacted OH and hydrophilic groups. As these agglomerates become surrounded by the PU matrix, the interaction of the moisture with the hygroscopic filler is increasingly restricted.

Morphological Characterization

Figure 4 shows the transmission optical micrographs of foams prepared with different formulations and cut parallel to the foaming direction. The higher glycerol [Figure 4(a–c)] or MNC [Figure 4(d–f)] contents seem to generate more fragile structures mainly denoted in the amount of broken cells. The cellulose particles affect the size and shape of the cells. The structure of cells became longer in the foam with cellulose, which is also denoted in the anisotropy index with values of 1.54 ± 0.15 for the unfilled foam and of 2.04 ± 0.14 for the foam with 3 wt % of cellulose.

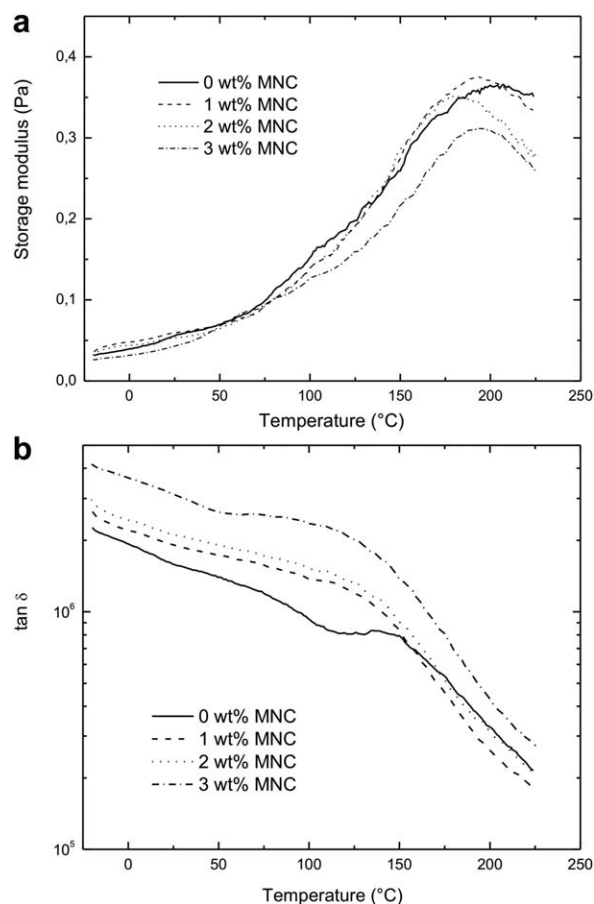


Figure 6. Storage modulus (a) and $\tan \delta$ (b) as a function of the temperature of foams modified with MNC.

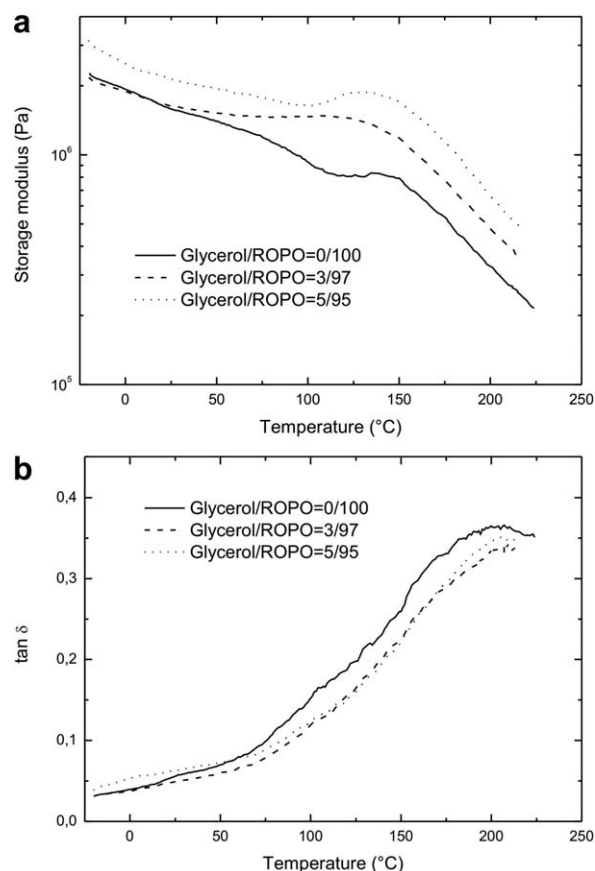


Figure 7. Storage modulus (a) and $\tan \delta$ (b) as a function of the temperature of foams modified with glycerol.

SEM of the specimens were also obtained and are shown in Figure 5. The samples were cut showing the longitudinal cross-sections that allow analyzing the profile of the foam.

The photos show foams with mostly closed cells and elongated in the growing direction. It can be seen that the increase of the glycerol content in the formulation did not reduce the homogeneity of the cell formation. The incorporation of MNC appears to slightly decrease the cell size. The broken walls of the cells generated during cutting are quite different in the samples with higher percentages of glycerol and MNC. The fragility in these samples increases as it was mentioned before. Some cellulose aggregates are observed in Figure 5(g) (indicated with arrows).

Mechanical and Dynamic-Mechanical Properties

Figures 6 (a,b) and 7(a,b) show storage modulus and $\tan \delta$ as a function of temperature for the dry foams modified with MNC and glycerol, respectively. The incorporation of the particles increases the modulus in the range of low temperatures denoting a reinforcing effect even for the very small added percentages of MNC [Figure 6(a)]. All the samples present glass transition temperatures higher than 170°C [Figure 6(b)]. The sample with 3 wt % of MNC seems to present a lower $\tan \delta$ peak than the other samples that could be related with a more heterogeneous network that is starting to be revealed at this percentage.

The replacement of ROPO by glycerol produces an increase in the rigidity of the foams denoted in higher storage modulus [Figure 7(a)]. Moreover, the glass transition temperature seems to start at higher temperatures as more glycerol is introduced in the foam formulation [Figure 7(b)]. These observations can be attributed to the increase in the crosslinking density with the glycerol incorporation.

To widen the characterization and corroborate the dynamic mechanical behavior, the mechanical properties of the ROPO/glycerol/PMDI were obtained by compression tests and the results are shown in Table IV. All the foams were tested by application of the compressive force in a parallel and perpendicular way to the growth direction of the foams. The replacement of ROPO by glycerol up to 3 wt % do not significantly modify the modulus when the foam is tested in the perpendicular way to the growth direction of the foams. A small increase in this property is observed in the formulation corresponding to glycerol/ROPO = 5/95. The stress at 10% of deformation tested in the direction of the foam growth increases with glycerol content.

When the foams are tested perpendicularly to direction of the foam growth, the replacement of ROPO with glycerol increases the compressive modulus, stress at 10% of deformation and yield; however, the yield deformation decreases.

These results could be correlated with an increase in the crosslinking density and in the rigidity of the structure with the addition of glycerol in the formulation (in agreement with DMA results). The isocyanate groups react with the hydroxyl groups of ROPO, glycerol, and water. The replacement of ROPO by glycerol that has a comparatively much higher hydroxyl value than the bio-polyol (1830 and 264.2 mg KOH/g

Table IV. Compression Properties of Foams Modified with Glycerol

Glycerol/ROPO weight ratio	Compression modulus (MPa) ^a	$\sigma_{10\%}$ of deformation (kPa) ^a	Compression modulus (MPa) ^b	$\sigma_{10\%}$ of deformation (kPa) ^b	σ_{yield} (kPa) ^b	$\varepsilon_{\text{yield}}$ (%) ^b
0/100	1.18 ± 0.27	56.2 ± 2.0	4.50 ± 0.67	156.8 ± 11.1	155.3 ± 15.1	4.60 ± 0.65
1/99	1.07 ± 0.11	61.7 ± 8.2	4.50 ± 0.41	163.8 ± 29.9	162.8 ± 34.5	4.09 ± 0.23
3/97	1.09 ± 0.16	72.3 ± 4.7	4.94 ± 1.11	165.0 ± 19.9	164.6 ± 28.1	4.22 ± 0.34
5/95	1.33 ± 0.03	87.5 ± 3.12	5.52 ± 0.41	172.6 ± 6.5	171.7 ± 9.2	4.07 ± 0.10

^a Compressive force applied perpendicular to the growth direction of the foams.

^b Compressive force applied parallel to the growth direction of the foams.

for the glycerol and ROPO, respectively) leads to the decrease of the chain mobility between crosslinks.

The comparison of the properties (modulus and stress at 10% of deformation) shows the expected results of better properties of the foams when the forces are applied parallel to the foam growth.

CONCLUSIONS

A natural ROPO was successfully synthesized and used in the formulation of a PU rigid foam using water as a reactive blowing agent. Commercial micro/nanocellulose was used as a filler while glycerol was applied as a reactive modifier that allowed to increase the crosslinking density in foamed PUs and to improve their mechanical properties.

The rigidity and glass transition temperatures increase with the incorporation of MNC and glycerol to the foam formulation as well as the water absorption and the fragility of the cell walls of the foams.

The considerable increase of foam compression strength, especially in the perpendicular direction to the foam growth, can be achieved by the modification of used PU systems with 5 wt % of glycerol, what is very important taking into account dimensional stability of foams containing natural oil-based polyols.

ACKNOWLEDGMENTS

The research leading to these results has received funding from the People Programme (Marie Curie Actions - International Research Staff Exchange Scheme) of the European Union's Seventh Framework Programme under REA grant agreement n° PIRSES-GA-2012-318996, titled "Bio-based polyurethane composites with natural fillers" (Acronym: BIOPURFIL). Thanks are also due to the Nac. University of Mar del Plata and CONICET from Argentina, and Cracow University of Technology from Poland.

REFERENCES

1. Woods, G. *The ICI Polyurethanes Book*, 2nd ed.; Wiley: NY, 1990.
2. Randall, D.; Lee, S. *The Polyurethanes Book*; Huntsman International LLC: UK, 2002.
3. Szycher, M. *Szycher's Handbook of Polyurethanes*; Taylor & Francis: USA, 2013.
4. Desroches, M.; Escouvois, M.; Auvergne, R.; Caillol, S.; Boutevin, B. *Polym. Rev.* **2012**, *52*, 38.
5. Chian, K. S.; Gan, L. H. *J. Appl. Polym. Sci.* **1998**, *68*, 509.
6. Khot, S. N.; Lascala, J. J.; Can, E.; Morye, S. S.; Williams, G. I.; Palmese, G. R.; Kusefoglou, S. H.; Wool, R. P. *J. Appl. Polym. Sci.* **2001**, *82*, 703.
7. Prociak, A. *Cell. Polym.* **2007**, *26*, 381.
8. Zlatanić, A.; Lava, C.; Zhang, W.; Petrović, Z. *S. J. Polym. Sci.: Part B: Polym. Phys.* **2004**, *45*, 809.
9. Mosiewicki, M. A.; Casado, U.; Marcovich, N. E.; Aranguren, M. I. *Polym. Eng. Sci.* **2009**, *49*, 685.
10. Petrovic, Z. S. *Polym. Rev.* **2008**, *48*, 109.
11. Rojek, P.; Prociak, A. *J. Appl. Polym. Sci.* **2012**, *125*, 2936.
12. Lozada, Z.; Suppes, G. J.; Tu, Y.-C.; Hsieh, F.-H. *J. Appl. Polym. Sci.* **2009**, *113*, 2552.
13. Kong, X.; Liu, G.; Qi, H.; Curtis, J. M. *Prog. Org. Coat.* **2013**, *76*, 1151.
14. Soykeabkaew, N.; Supaphol, P.; Rujiravanit, R. *Carbohydr. Polym.* **2004**, *58*, 53.
15. Marcovich, N. E.; Reboredo, M. M.; Aranguren, M. I. *J. Appl. Polym. Sci.* **1998**, *70*, 2121.
16. Bledzki, A. K.; Zhang, W.; Chate, A. *Compos. Sci. Technol.* **2001**, *61*, 2405.
17. Silva, R. V.; Spinelli, D.; Bose Filho, W. W.; Claro Neto, S.; Chierice, G. O.; Tarpani, J. R. *Compos. Sci. Technol.* **2006**, *66*, 1328.
18. Saliba, C. C.; Oréfice, R. L.; Carneiro, J. R. G.; Duarte, A. K.; Schneider, W. T.; Fernandes, M. R. F. *Polym. Test.* **2005**, *24*, 819.
19. Cotgreave, T. C.; Shortall, J. B. *J. Mater. Sci.* **1977**, *12*, 708.
20. Barma, P.; Rhodes, M. B.; Salover, R. *J. Appl. Phys.* **1978**, *49*, 4985.
21. Marcovich, N. E.; Bellesi, N. E.; Auad, M. L.; Nutt, S. R.; Aranguren, M. I. *J. Mater. Res.* **2006**, *21*, 870.
22. Goods, S. H.; Neuschwanger, C. L.; Whinnery, L. L.; Nix, W. D. *J. Appl. Polym. Sci.* **1999**, *74*, 2724.
23. Vaidya, N. Y.; Khakhar, D. V. *J. Cell. Plast.* **1997**, *33*, 587.
24. Siegmann, A.; Kenig, S.; Alperstein, D.; Narkis, M. *Polym. Compos.* **1983**, *4*, 113.
25. Mosiewicki, M. A.; Dell'arciprete, G. A.; Aranguren, M. I.; Marcovich, N. E. *J. Compos. Mater.* **2009**, *43*, 3057.
26. Jin, J. F.; Chen, Y. L.; Wang, D. N.; Hu, C. P.; Zhu, S.; Vanoverloop, L.; Randall, D. *J. Appl. Polym. Sci.* **2002**, *84*, 598.
27. John, J.; Bhattacharya, M.; Turner, R. B. *J. Appl. Polym. Sci.* **2002**, *86*, 3097.
28. Hu, Y. H.; Gao, Y.; Wang, D. N.; Hu, C. P.; Zhu, S.; Vanoverloop, L.; Randall, D. *J. Appl. Polym. Sci.* **2002**, *84*, 591.
29. Urbanski, J. In *Handbook of Analysis of Synthetic Polymers and Plastics*; Urbanski, J., Czerwinski, W., Janicka, K., Majewska, F., Zowall, H., Eds.; Wiley: Poland, 1977; Chapter 1, Section 1.2, pp 48–54.
30. Sernek, M.; Kamke, F. A. *Int. J. Adhes. Adhes.* **2007**, *27*, 562.